

# Independent component analysis with ball-stick model tractography to solve an intra-voxel crossing fiber problem in clinical DTI data

Jeong-Won Jeong<sup>1,2</sup>

<sup>1</sup>Pediatrics and Neurology, Wayne State University, Detroit, Michigan, United States, <sup>2</sup>PET center, Children's Hospital of Michigan, Detroit, Michigan, United States

**Targeted audience:** Clinical researchers using diffusion tensor imaging. **Purpose:** Recently, an independent component analysis with ball-stick model (ICA+BSM)<sup>1</sup> was proposed to solve an intra-voxel crossing fiber problem in diffusion tensor imaging (DTI). The present study investigates whether the ICA+BSM analysis can estimate accurate orientation of multiple fiber bundles in clinical DTI data, typically sampling the displacement of water diffusion at a single shell with relatively low angular resolution (e.g., b-value =1000 s/mm<sup>2</sup> and number of encoding directions < 60).

**Methods:** By varying b-value (1000-3000 s/mm<sup>2</sup>) and the number of encoding gradients, g (6-150), a series of simulation data were generated at a local cluster of 27 voxels (i=1,2,...,27) by using conventional ball-stick model<sup>2</sup> where diffusion measurement at the i<sup>th</sup> voxel crossing K-fibers,  $s_i(b,g)$  is defined by a linear summation of a single isotropic compartment ( $D_{i0}$ ) and K- anisotropic stick compartments ( $D_{ij}$ ):  $s_i(b,g) = (1 - \sum_{j=1}^K f_{ij})\exp(-bg^T D_{i0}g) + \sum_{j=1}^K f_{ij}\exp(-bg^T D_{ij}g)$ ,  $D_{i0} = E_0 V_0 E_0^T$ ,  $D_{ij} = E_j V_j E_j^T$  where  $E_0 = \text{diag}(1,1,1)$ ,  $E_j$  = a vector with unit norm,  $V_0 = \text{diag}(\lambda_1, \lambda_1, \lambda_1)$ ,  $V_j = \text{diag}(\lambda_1, \lambda_2, \lambda_3)$ ,  $[\lambda_1, \lambda_2, \lambda_3] = [1.7, 0, 0] \times 10^{-3} \text{mm}^2/\text{s}$ . For K=2, the crossing angle (called "inter-fiber angle") was randomly selected from 10° to 80° to generate two  $E_{j=1,2}$ . For K=3, the two inter-fiber angles were assumed to be equal to simulate three  $E_{j=1,2,3}$ . The volume fraction,  $f_{ij}$ , were randomly assigned in the range from 0.1 to 0.9 such that  $\sum f_j = 1$ . A total of 1000 trials per each of the inter-fiber angles were

repeated for each mixture of two and three fibers. The accuracy of recovering fiber orientations was evaluated by the absolute angular error between the actual orientation (1st eigenvector of simulated  $D_j$ ) and the estimated tensor orientation (1st eigenvector of recovered  $D_j$ ) obtained from the ICA+BSM analysis. Also, to assess how accurately the ICA+BSM can resolve the orientation of crossing fibers compared with other high angular resolution diffusion imaging (HARDI) such as Q-ball imaging (QBI), diffusion spectrum imaging (DSI), generalized Q-ball imaging (GQI)<sup>3</sup>, we utilized an in-vivo spindle data<sup>4</sup> with interleaved 90° crossing of two fibers (available from NIH NITRC database at [http://www.nitrc.org/frs/?group\\_id=627](http://www.nitrc.org/frs/?group_id=627)). Finally, the performance of ICA+BSM was assessed using two 3 Tesla DTI data (12 and 55 encoding gradients at b=1000 s/mm<sup>2</sup>) obtained from a 20 year-old healthy adult. Three fiber pathways of interest, corpus callosum (CC), arcuate fasciculus (AF), and cortico-spinal tract (CST), intermingling over the lateral region of central gyrus/sulcus, were investigated to demonstrate the feasibility of ICA+BSM at clinical DTI data. **Results:** Simulation studies assessing the absolute error for two and three fibers per voxel demonstrated that the ICA+BSM provides promising accuracy (Fig. 1, median value of error angle = 4.1° and 10.4° for K=2 and 3, respectively) even at small b-value (=1000 s/mm<sup>2</sup>) and small number of encoding gradients (=12). More interestingly, compared with DSI, QBI, and GQI, the ICA+BSM provides the most reliable recovery of multiple fiber directions even in single shell low angular acquisition (55 encoding gradients at b=1000 s/mm<sup>2</sup>, Fig. 2 c). The superior performance of ICA+BSM over other methods may be explained by the fact that the ICA+BSM fits multiple fibers with independent diffusion processes observed in the cluster of multiple voxels, specifically, the crossing fiber tracts such as CC, AF, and CST can be resolved at clinical DTI data using the information from the cluster of neighboring voxels (Fig. 3).

**Figure 1.** Error angle between actual and estimated fibers for two (K=2) and three (K=3) cylindrical fibers. Each box plot consists of median (red), quartiles (blue), and total extent of errors (black dotted).

**3). Discussion and Conclusion:** A key novelty of ICA+BSM is that it isolates independently attenuated diffusion profiles from "neighboring voxels" to optimize initial guesses of multiple fiber components existing in a single voxel. In-vivo, the crossing of prominent fiber tracts is most likely observable in the cluster of neighboring voxels. Thus, the independent diffusion processes existing in the cluster can be better estimates of multiple

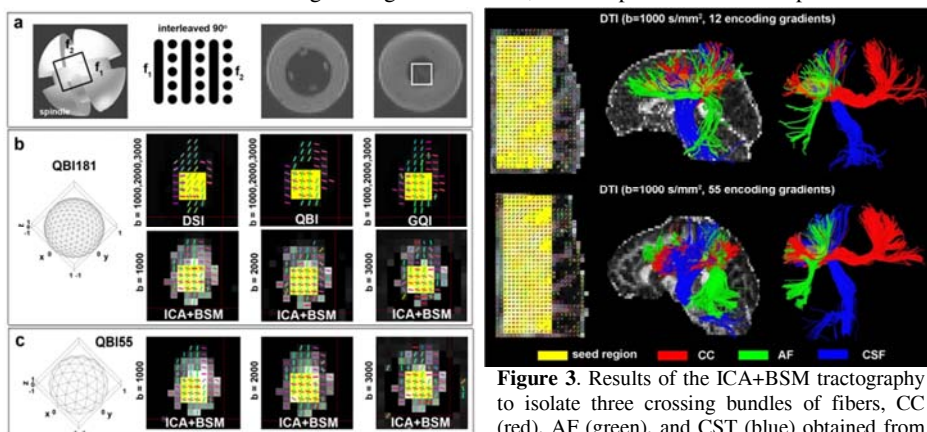


**Figure 2.** (a) In-vivo phantom used. (b) Fiber orientation maps obtained from DSI, QBI, GQI, and ICA+BSM (181 encoding gradients). (c) Fiber orientation maps obtained from ICA+BSM (55 encoding gradients). Yellow box indicates the voxels of crossing two fibers,  $f_1$  and  $f_2$ .

fibers compared to those multiple fibers observed in a single voxel, that is feasibly suited to be trapped at local minimum and also require computational complexity in the overall fitting procedure. The ICA+BSM method effectively solves an intra-voxel problem and helps to better visualize the underlying white matter architecture in clinical DTI data.

**References:** 1. Jeong JW, Asano E, Yeh FC, et al. Independent component analysis tractography combined with a ball-stick model to isolate intra-voxel crossing fibers of the corticospinal tracts in clinical diffusion MRI. Magn Reson Med. 2013;70:441-53. 2. Schultz T, Westin CF, Kindlmann G. Multi-diffusion-tensor fitting via spherical deconvolution: a unifying framework. Med Image Comput Comput Assist Interv 2010;13(Pt 1):674-81. 3. Yeh FC, Wedeen VJ, Tseng WY. Generalized q-sampling imaging. IEEE Trans Med Imaging 2010;29:1626-1635. 4. Moussavi-Biugui A, Stieltjes B, Fritzsche K, et al. Novel spherical patters for Q-ball imaging under in vivo conditions. Magn Reson Med. 2011; 65:190-94.

**Figure 3.** Results of the ICA+BSM tractography to isolate three crossing bundles of fibers, CC (red), AF (green), and CST (blue) obtained from clinical DTI data (top: b=1000 s/mm<sup>2</sup>, 12 encoding gradients, bottom: b=1000 s/mm<sup>2</sup>, 55 encoding gradients). Yellow indicates seed regions at the lateral region of central gyrus/sulcus. It is clear that three pathways are discernible even in 12 encoding gradients.